Energy Informatics

RESEARCH

Open Access

Comprehensive testing technology for new energy vehicle power batteries based on improved particle swarm optimization

Hongxing Liu[1*] and Yi Liang[1]

*Correspondence:
liuhongxing2023@126.com

[1] School of Automobile Engineering, Guilin University of Aerospace Technology, Guilin 541004, China

Abstract

As the new energy industry continues to progress, the health management of power batteries has become the key to ensuring the performance and safety of automobiles. Therefore, accurately predicting battery capacity decline is particularly important. A battery capacity degradation prediction model combining unscented particle filtering, particle swarm optimization, and SVR is constructed. It optimizes regression parameters through the introduced optimization strategy. Unscented particle filtering is used to improve particle swarm optimization and battery detection model. The study tested four various models of lithium-ion batteries. The model predicted a mean square error of 0.0011 for battery 5, 0.0007 for battery 6, 0.0022 for battery 7, and 0.0013 for battery 18. In the prediction of different battery types, the mean square error of the NIMH battery was reduced by 0.0008 compared with the particle swarm optimization-support vector regression algorithm, and by 0.0005 compared with the unscented particle filtering-regression vector regression algorithm. The mean square error of lithium-iron phosphate battery was reduced by 0.0008 and 0.0004 respectively compared with comparison models. The mean square error value of lithium titanate battery was reduced by 0.0007 and 0.0003 respectively in the research model compared with comparison models. It improves the prediction accuracy in lithium-ion batteries. Its application in battery health management can provide important technical support for improving battery performance and extending service cycles. The proposed method can be used for battery monitoring and management of power grid energy storage system. By accurately predicting the capacity decline of battery, the operation strategy of energy storage system can be optimized to ensure the efficient operation and long life of the system. The battery management system can be used for drones and aviation equipment to predict battery health and capacity decline in real time, ensuring the safety and reliability of flight missions.

Keywords: Unscented particle filtering, Particle swarm optimization algorithm, SVR, Lithium-ion batteries, Life prediction

Introduction

With the changing global energy structure and increasing environmental requirements, new energy vehicles are rapidly becoming the development direction of the future automotive industry. As the core component, the power of batteries directly affects the

vehicle's endurance, safety, and economy. Lithium-ion Battery (LB) is the mainstream choice for power batteries due to its high energy density, and good electrochemical performance (Che et al. 2023; Kong et al. 2022). However, as the usage time increases, the battery performance will gradually decline. This seriously affects the service life and safety performance of the vehicle. Therefore, how to accurately predict battery capacity degradation has become an urgent technical challenge. At present, the research on battery health management systems mainly focuses on predicting battery capacity and internal resistance attenuation. Among them, machine learning prediction methods have received widespread attention due to their ability to handle nonlinear problems. Especially, support vector machines, neural networks, and regression analysis methods have shown excellent performance in battery life prediction (Guo et al. 2023; Liu et al. 2022). Accordingly, they typically need rich historical data to train the model. In addition, their stability and accuracy in dealing with data with significant uncertainty still need to be improved. Therefore, a comprehensive prediction model consisting of Unscented Particle Filtering (UPF), Particle Swarm Optimization (PSO), and Support Vector Regression (SVR) is proposed. It is expected to improve the prediction accuracy and stability of capacity degeneration in LB. UPF is an advanced filtering method, combining the advantages of Unscented Kalman filter (UKF) and Particle Filter (PF). UPF can effectively deal with nonlinear and non-Gaussian noise problems. In the battery capacity decline prediction, UPF is able to update and adjust the prediction model in real time, deal with noise and uncertainty in the data, and enhance prediction reliability. PSO is a global optimization algorithm based on swarm intelligence, which seeks the optimal solution by simulating the foraging behavior of birds. PSO has strong global search ability, simple implementation and few parameters. In the prediction of battery capacity decline, PSO can be used to optimize the parameter combination of SVR to improve the prediction performance of the model. SVR is a regression method based on statistical learning theory. By introducing kernel function technique, SVR can deal with complex non-linear relations, which has good generalization ability. In the prediction of battery capacity decline, SVR controls the model complexity through the principle of structural risk minimization to prevent over-fitting. The research innovation lies in proposing a multi-algorithm combination prediction model. PSO optimizes the parameters of the SVR model to adapt to different battery data characteristics. It is a new attempt in the battery life prediction. The research has four parts. The first summarizes the research achievements on PSO and battery testing technology. The second part builds a predictive model for the lifespan decline of LB. The third part conducts performance and application testing on the constructed model through relevant datasets. The last summarizes the results, existing problems and future research directions.

With the advancement of new energy vehicles, the life testing of automotive power batteries has become a focus. The current mainstream method for predicting lifespan is based on models constructed using PSO. Mao et al. developed a dual group collaborative PSO to recognize noise immunity in LB. The deviation was reduced by 35 dB. It exceeded existing methods in terms of noise resistance, reliability, and accuracy (Mao et al. 2022). Zhang et al. proposed an improved PSO for extreme learning machine neural networks. The algorithm had mean square errors of 0.31%, 0.32%, and 0.14% for battery charging state in mixed pulse power characteristics, Beijing bus dynamic stress

testing, and dynamic stress testing conditions, respectively. The proposed algorithm solved the poor accuracy in battery SOC estimation in the past (Zhang et al. 2022). Ra et al. developed a power loss optimization method for the battery storage system based on PSO technology. This method maximized the efficiency of the overall battery system (Ra et al. 2022). Sevilgen et al. used PSO to optimize the liquid cooling system of battery modules. The results showed that the proposed algorithm reduced pump power consumption by 22.4% while maintaining cooling performance (Sevilgen et al. 2022).

Xiong et al. proposed a fusion model that combined correlation coefficient and Relief. The study used two types of lithium batteries for battery health estimation. The estimation accuracy of this model was improved by 63.5% and 71.1% in two types of lithium batteries, respectively (Xiong et al. 2023). Sun et al. built a battery life prediction model based on health feature parameters. This method combined empirical mode decomposition, incremental capacity analysis, and gated recursive units. The study aimed to validate the NASA lithium battery dataset. The error was 0.3% (Sun et al. 2022). Ma et al. built a framework to achieve real-time health prediction of invisible battery. It achieved an average testing error of 0.176% and 8.72% in capacity estimation and remaining service life prediction (Ma et al. 2022). Hu et al. proposed an attention-based LB calendar health prediction model. It achieved good domain complementarity based on battery experience knowledge. In experiments on actual battery calendar aging, this method outperformed other prediction strategies in predicting and generalizing unknown conditions (Hu et al. 2022).

In summary, although there have been some achievements in current research on battery health detection, the above methods mainly rely too much on precisely defined model parameters and algorithm optimization. This inevitably limits the generalization ability in facing real and complex environments. Moreover, these studies still show certain limitations in dealing with the uncertainty and noise of battery data, which may affect the prediction accuracy. To address current shortcomings, the study adopts UPF to handle the uncertainty and noise of battery data. Then a combined model UPF-PSO-SVR based on the parameter optimization ability of PSO is proposed.

Construction of automotive power battery testing model based on improved PSO

The study focuses on the comprehensive testing of power batteries for new energy vehicles. Firstly, a life decline prediction model for LB is constructed using PSO. The batteries are tested from the perspective of battery health. Next, to address the shortcomings of PSO, the UPF algorithm is introduced to improve PSO. Finally, an SVR model is introduced to construct a health prediction model for new energy vehicle power batteries. This combined model is chosen because the three methods complement each other. UPF performs well in filtering noise, deals with non-linear and non-Gaussian problems, and provides more accurate and stable data input for SVR. PSO provides global optimal parameter setting for SVR, which improves the prediction performance and accuracy of SVR. SVR improves the overall performance of the prediction model by capturing complex non-linear relationship in battery capacity decline through kernel function technique.

Construction of degeneration model for LB

LB has extensive applications in daily life. For example, as a power battery in new energy vehicles, the lifespan of new energy vehicles is related to the quality of LB. The anode of LB is lithium oxide. The cathode is carbon material with micro-pores. During battery operation, the anode decomposes lithium ions, while the cathode accommodates the decomposed ions. In an electrolyte solution, a high concentration of lithium ions indicates a large storage capacity inside the lithium battery. During the battery charging, the current is around 0.2C–1C. If the current is high, the internal chemical reaction is more intense. It causes the battery heating (You et al. 2022). Its working state is displayed in Fig. 1 (Zhang and Zhao 2023).

In Fig. 1, lithium ions move back and forth between the two poles. At this point, there is electrolyte solution and membrane loss inside the battery. Moreover, external environmental factors can affect battery cycling and lead to irreversible degradation. Therefore, during continuous operation, the performance will deteriorate. Before the battery is completely damaged, it is necessary to predict its lifespan to prevent accidents from occurring. LB has the non-linear capacity degradation in life prediction. Therefore, conventional battery health assessment may lack accuracy (Nsugbe 2023; Cao et al. 2023). The study uses a double exponential empirical degradation strategy to represent the battery degradation model, as shown in formula (1).

$$Q_k = a * \exp(b * k) + c * \exp(d * k) \tag{1}$$

In formula (1), Q_k stands for the battery power. k represents the cycles of lithium ions. a and c stand for parameters of battery resistance. b and d are parameters of the battery capacity decline rate. Formula (1) is used to quantify the capacity decline of the battery. It provides a basis for the subsequent model construction. To make the degradation model more closely fit the actual value of battery capacity degradation, the state and observation formulas of the prediction model are presented in formula (2).

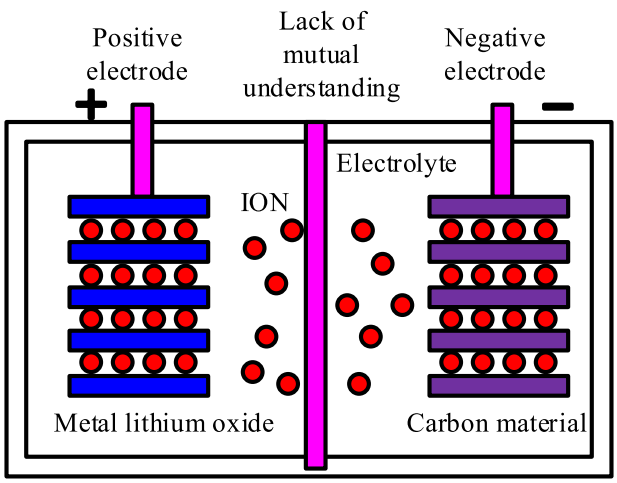

Fig. 1 Working state of LB

$$\begin{cases} X(k) = \left[a(k)\ b(k)\ c(k)\ d(k) \right] \\ a(k+1) = a(k) + w_a(k), w_a \sim N(0, \sigma_a) \\ b(k+1) = b(k) + w_b(k), w_b \sim N(0, \sigma_b) \\ c(k+1) = c(k) + w_c(k), w_c \sim N(0, \sigma_c) \\ d(k+1) = d(k) + w_d(k), w_d \sim N(0, \sigma_d) \\ Q_k = a(k) \exp(b(k) * k) + c(k) \exp(d(k) * k) + v(k) \end{cases} \tag{2}$$

In formula (2), $v(k)$ is the Gaussian white noise. w represents the observation noise. σ represents the variance. Formula (2) is used to represent the relationship between the actual observed value and the model predicted value, taking into account the effect of noise on the observed result. In general, the PSO algorithm can be applied to solve the degradation prediction model constructed above. The PSO is a heuristic optimization algorithm that uses particles to search in the search space. Particles continuously updates their position and velocity to complete the optimal value solution (Pervaiz et al. 2022). In the battery life prediction model, the PSO can be applied to optimize parameters. The PSO algorithm updates particles in a specific way, as shown in formula (3).

$$\begin{cases} V_k^i = \omega V_{k-1}^i + \mu_1 Rand(0,1)(P_{best}^i - X_{k-1}^i) + \mu_2 Rand(0,1)(G_{best} - X_{k-1}^i) \\ X_k^i = X_{k-1}^i + V_k^i \end{cases} \tag{3}$$

In formula (3), V_k^i represents the particle velocity. X_k^i stands for the particle position. $Rand(\cdot)$ stands for a random number selection function, with the value ranging from 0 to 1. ω represents the inertia factor. μ_1 represents the learning factor. There is a positive correlation between the value of ω and the global search ability of PSO. G_{best} represents the global optimum. P_{best}^i represents the individual optimum. During the particle update process, PSO uses G_{best} and P_{best}^i as references and updates them through formula (3). Particles have a certain directionality. Particles approach particles with higher weights. From a macroscopic perspective, the weight of more particles will increase, while the variance of particle weights will decrease. These parameters together determine the motion mode of particles in the search space and the search efficiency. By adjusting these parameters, global search and local search capabilities can be balanced. The convergence speed and the quality of the algorithm can be improved. Formula (3) is used to optimize the model parameters, so that the battery degradation model can predict the battery life more accurately. Therefore, PSO is combined with UPF to address the particle degradation. The PSO-UPF combination model mainly improves the fitness function and granular updating mechanism. Among them, the model defines a fitness function according to the characteristics of the PSO optimization algorithm, as shown in formula (4). It makes particle updates closer to particles with higher weights.

$$f = \exp\left[-\frac{1}{2R_k} (Z_k - \hat{Z}_k^i)^2 \right] \tag{4}$$

In formula (4), Z_k represents the particle observation value at the current time. $\hat{Z}_k^i$ represents the particle's predicted value. R_k represents the observed noise's covariance. Formula (4) is used to evaluate the merits and demerits of particles. In the optimization process, the fitness function is minimized to improve the prediction accuracy of the model. The model evaluates the fitness of each particle by calculating the error between the current particle position and the actual observation data. Formula (4) gives

this assessment and adds a penalty factor to prevent over-fitting. According to the fitness function value, the PSO algorithm adjusts the speed and position of each particle to gradually approach the optimal solution. In each iteration, the PSO algorithm tracks the individual optimal position and the global optimal position for each particle. The fitness function values are compared to determine whether to update these optimal positions. In the whole optimization process, PSO algorithm is integrated with the battery capacity degeneration model. The prediction accuracy is improved by continuously optimizing the model parameters. Ultimately, the optimized parameters are used to build a more accurate battery capacity prediction model. In the particle update mechanism, the model has a Gaussian distribution function to update the velocity and position. The update method is replaced with fixed velocity and inertia factors. This method enhances the diversity while retaining the inherent convergence characteristics of the PSO algorithm. Therefore, the particle update is shown in formula (5).

$$\begin{cases} V_{k-1}^{i} = \left|Ramdn_1(0,1)\right|(P_{best}^{i} - X_{k-1}^{i}) + \left|Ramdn_2(0,1)\right|(G_{best}^{i} - X_{k-1}^{i}) \\ X_{k}^{i} = X_{k-1}^{i} + V_{k-1}^{i} \end{cases} \tag{5}$$

In formula (5), $\left|Ramdn(0,1)\right|$ represents a positive random digit that satisfies a Gaussian distribution. In formula (5), random numbers satisfying Gaussian distribution are added in the process of particle renewal to enhance the diversity of particle population, retain the inherent convergence characteristics, and weakens the degradation effect. According to formula (5), global particles can continuously move towards the real state region, gradually approaching the real state, and enhancing the tracking performance. However, the model is constrained by internal factors of the battery and external environment. The particle degradation phenomenon has uncertain information. Therefore, the study uses UPF algorithm to improve the PSO model and achieve battery life prediction. The flowchart of the UPF-PSO model is shown in Fig. 2 (Zhi et al. 2022).

In Fig. 2, particle initialization is first completed through PSO. $p(X_0)$ is used as the initial prior probability distribution. The initialization state set of particles is obtained by selecting particles from $p(X_0)$, denoted as X_0^i. $w_0^i = \frac{1}{N}$ represents the initial weight of the particle. The second step of UPF is to suggest sampling the probability density distribution. In this stage, the extended Kalman filtering is applied to update the sampling points. This operation obtains the suggested distribution function, updates the

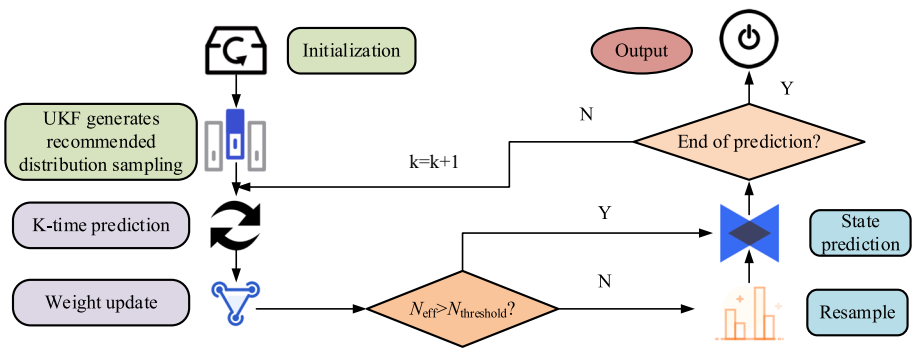

Fig. 2 UPF-PSO flowchart

weights, and normalizes the particle weights. The third step is the resampling stage, which involves resampling the particle set to obtain a new one. The fourth step is to perform state estimation and variance output in the new particle set. The UPF algorithm constructed above can effectively solve the particle degradation phenomenon limiting the accuracy of predicting battery life. However, this algorithm still generates inevitable and undeniable errors in filtering iterative prediction. Therefore, further error correction is adopted in research to optimize the accuracy and stability.

Battery testing model based on UPF-PSO-SVR

The study introduces SVR into the model. It aims to find the optimal hyperplane in non-linear regression problems to best fit the given training data. Unlike traditional regression methods, SVR not only focuses on the prediction accuracy of points, but also on the minimum distance between the boundary between the model and the training samples. For specific regression problems, SVR first represents the training dataset with $\{x_i, y_i\}_{i=1}^{n}$, where the two elements are the input feature vector and the output target quantity. The formed regression model should be as close to the output as possible. Its equation expression is shown in formula (6).

$$f(x) = w^T \phi(x) + B \tag{6}$$

In formula (6), $\phi(x)$ represents a non-linear function. B represents the bias vector. Formula (6) is used to construct the SVR model and find the optimal hyperplane to fit the training data in the non-linear regression problem. There are some differences between SVR and traditional regression models, because SVR allows for a certain degree of error in the regression model and the real data. This error is recorded as ε. From this, SVR actually minimizes structural risk. Therefore, it is represented by formula (7) to minimize structural risk.

$$\begin{cases} \min \frac{\|w\|^2}{2} + C \sum_{i=1}^{n} (\xi_i + \hat{\xi}_i) \\ s.t. \begin{cases} f(x_i) - y_i \le \varepsilon + \xi_i \\ y_i - f(x_i) \le \varepsilon + \hat{\xi}_i \\ \xi_i \ge 0, \hat{\xi}_i \ge 0, i = 1, 2, ..., n \end{cases} \end{cases} \tag{7}$$

In formula (7), C stands for the penalty factor, which balances the model's generalization ability and classification accuracy. $\|w\|^2$ shows the complexity of the model. ξ_i represents the relaxation factor. Formula (7) optimizes the SVR model to ensure good prediction accuracy while ensuring generalization ability. The Lagrange function is used to solve formula (7), as shown in formula (8).

$$\begin{aligned} L(w, B, \alpha, \hat{\alpha}, \xi, \hat{\xi}, \mu, \hat{\mu}) = {} & \frac{1}{2}\|w\|^2 + C \sum_{i=1}^{n} (\xi_i + \hat{\xi}_i) - \sum_{i=1}^{n} \mu \xi_i - \sum_{i=1}^{n} \hat{\mu} \hat{\xi}_i \\ & + \sum_{i=1}^{n} \alpha_i (f(x_i) - y_i - \varepsilon - \xi_i) + \sum_{i=1}^{n} \hat{\alpha}_i (y_i - f(x_i) - \varepsilon - \hat{\xi}_i) \end{aligned} \tag{8}$$

In formula (8), μ and α are both Langrange day multipliers. Formula (8) transforms the original problem into a dual problem to optimize the regression model by solving the Lagrange function. The first step of the Lagrange derivation process is to take the partial derivative of the Lagrange function and set the function as 0 to eliminate the Lagrange multiplier. In the second step, the dual problem is constructed. The kernel function is used to deal with the high-dimensional feature space, so as to solve the non-linear regression problem effectively. The dual function is shown in formula (9).

$$f(x) = \sum_{i=1}^{n} (\hat{\alpha}_i - \alpha_i) K(x_i, x_j) + B \tag{9}$$

In formula (9), K stands for the kernel function of the regression model. $(\hat{\alpha}_i - \alpha_i)$ stands for the support vector. The radial basis kernel function is used to study kernel functions, mapping input data to high-dimensional feature spaces, and thus handling nonlinear problems. In practical applications, the number of support vectors is much smaller than the total number of samples, so as to ensure the sparsity and efficiency of the model. Formula (9) is used for the final regression model solution. The kernel function is used to deal with the non-linear problem and predict the battery capacity. The penalty factor and kernel function parameters are the two most crucial parameters in the SVR. The improved model can be used for actual battery capacity prediction. The filtered state space equation is represented by formula (10) according to formula (1).

$$\begin{cases} x_{k+1} = x_k + w_k \\ y_k = a_k * \exp(b_k * k) + c_k * \exp(d_k * k) + v_k \end{cases} \tag{10}$$

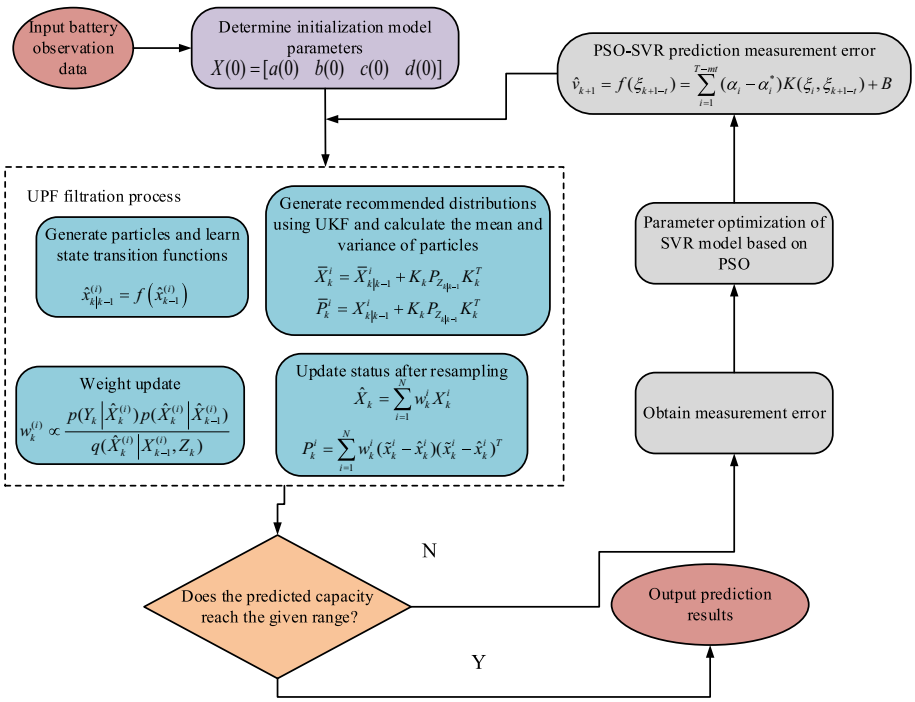

Fig. 3 Prediction process of battery capacity decline based on fusion model

From formula (10), v_k cannot be avoided throughout the battery degradation prediction process. Formula (10) is used to describe the dynamic process of battery capacity degradation, which is filtered and predicted by state transition and observation formula. Therefore, it can only reduce the overall impact of errors on the model. The process of using PSO-SVR to reduce observation errors is shown in Fig. 3 (Du et al. 2022).

Figure 3 displays the overall process. The first step is to input battery observation data to determine the initial model parameters. Secondly, UPF is carried out. The filtering process includes generating particles and learning state transition function. The UKF is used to generate recommendation distribution, calculate mean and variance of particles, and update weight and status after resampling. Then, it is judged whether the prediction capacity reaches the given range. If it reaches the given range, the result is output. If it does not reach the given range, the measurement error is obtained. PSO is adopted to optimize the parameters. Finally, the measurement error is obtained and the filtering operation is performed again (Du et al. 2022).

The model initialization is as follows: determine the prediction starting point and set the prediction time point to T. Before T, the cycle cycles obtained by the model are used as training set data. The data obtained after T is the testing set data. The initial parameters are determined using a sparse vector machine. The expression is shown in formula (11).

$$X(0) = \left[a(0)\ b(0)\ c(0)\ d(0) \right] \tag{11}$$

Formula (11) is used to determine the initial parameters of the SVR model. The sparse vector machine is used to obtain the initial value of the model, which provides the basis for the subsequent prediction. The UPF process includes generating particles, learning state transition functions, generating recommendation distributions, calculating the average and variance of particles, updating weights, and updating the state after resampling. This step can be represented by formula (12).

$$\begin{cases} \hat{x}_{k|k-1}^{(i)} = f\left(\hat{x}_{k-1}^{(i)}\right) \\ \begin{cases} \overline{X}_k^i = \overline{X}_{k|k-1}^i + K_k P_{Z_{k|k-1}} K_k^T \\ \overline{P}_k^i = X_{k|k-1}^i + K_k P_{Z_{k|k-1}} K_k^T \end{cases} \\ w_k^{(i)} \propto \frac{p(Y_k \left| \hat{X}_k^{(i)} \right.) p(\hat{X}_k^{(i)} \left| \hat{X}_{k-1}^{(i)} \right.)}{q(\hat{X}_k^{(i)} \left| X_{k-1}^{(i)}, Z_k \right.)} \\ \begin{cases} \hat{X}_k = \sum_{i=1}^{N} w_k^i X_k^i \\ P_k^i = \sum_{i=1}^{N} w_k^i (\tilde{x}_k^i - \hat{x}_k^i)(\tilde{x}_k^i - \hat{x}_k^i)^T \end{cases} \end{cases} \tag{12}$$

In formula (12), $\overline{X}_k^i$ represents calculating the mean of particles. $\overline{P}_k^i$ represents calculating the variance of particles. Formula (12) is used to update and evaluate the particle state and improve the filtering accuracy. The particle resampling is displayed in Fig. 4 (Du et al. 2022).

In Fig. 4, the particle size represents the corresponding weight. Before resampling, the weights of particles are unevenly distributed. After resampling, particle sets with equal weights can be obtained. In the prediction observation error stage of the model, an observation time point is set, denoted as T. The observation error data before T is used as training

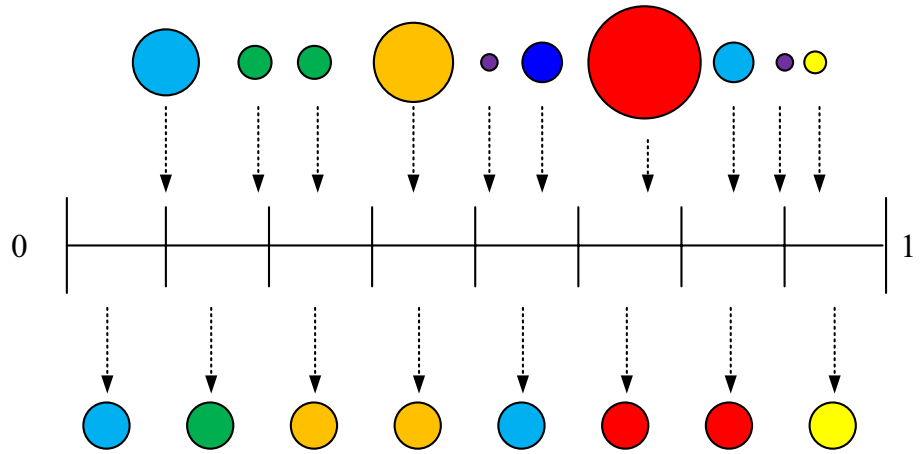

Fig. 4 Process of particle resampling

set of the model to correct subsequent errors. Therefore, an SVR model for observing the error before time T is established. The specific expression of this model is shown in formula (13).

$$\eta_k = f(\xi_k) = \sum_{i=1}^{T-m} (\hat{\alpha}_i - \alpha_i) K(\xi_i, \xi_k) + B \tag{13}$$

In formula (13), η_k stands for the SVR model. ξ stands for the relaxation factor. $(\hat{\alpha}_i - \alpha_i)$ represents the support vector of the model. B represents the bias vector. K represents the kernel function. Formula (13) trains the model using the observation errors before the predicted time point, and predicts the observation errors at the predicted time point. Then the corresponding SVR model is established to provide a prediction framework for subsequent observation errors. After training with formula (13), the observation error of the model is corrected. The corrected observation error can be represented by formula (14).

$$\hat{v}_{k+1} = f(\xi_{k+1-t}) = \sum_{i=1}^{T-mt} (\alpha_i - \alpha_i^*) K(\xi_i, \xi_{k+1-t}) + B \tag{14}$$

In formula (14), $\hat{v}_{k+1}$ represents the predicted observation error value at the predicted time point. Formula (14) predicts and corrects the observation error by SVR model to further improve the prediction accuracy. In the above process, the UPF-PSO-SVR fusion algorithm is proposed. The SVR algorithm utilizes the degradation information at the previous moment and the filtering results, effectively reducing the influence of observation noise. At the same time, PSO is adopted to optimize the SVR penalty coefficient C, as well as kernel function parameter γ. The state update method of the UPF algorithm is modified to compensate for the inability of the UPF algorithm to obtain real data after the set prediction time point. The battery status is determined by the first set battery failure range. If the predicted capacity reaches the battery failure range, the remaining service life is taken as the distinctions between

the forecast cycle period T and the failure period. If the failure range is not met, the error is further predicted and updated.

Performance verification of battery capacity degradation model based on UPF-PSO-SVR

To display how the constructed model performs, a comprehensive test is conducted on LB using the model. Four different LBs are selected for testing in the experiment. The model is assessed using the Mean Absolute Error (MAE) and Root Mean Square Error (RMSE) in the actual and the test value. Uncertainty analysis and error analysis are conducted to predict the probability distribution of the results. The health status of battery performance and the correlation between health characteristics are analyzed.

Performance analysis of the improve model

The experiment is conducted using the Battery Date Set dataset, which is provided by the Aerospace Excellence Fault Prediction Center. The dataset contains relevant data for batteries 5#, 6#, 7#, and 18#. The first three groups of batteries have 179 sets of cycle data, and the last group of batteries has 143 sets of cycle data. The initial parameters are appeared in Table 1.

The study validates the improved model in the experimental environment mentioned above. Unscented Particle Filter-SVR (UPF-SVR) and Unscented Particle Filter-Regression Vector Regression (UPF-RVR) are used as comparative models to test batteries 5#, 6#, 7#, and 18#, respectively (Meng et al. 2023). The results are shown in Fig. 5.

Figures 5a and b represent the prediction for 60 and 100 cycles of battery 5#, respectively. Figures 5c and d represent predictions for 60 and 100 cycles of battery 6#. Figures 5e and f respectively represent prediction for 60 and 100 cycles of battery 7#. Among them, the RMSE value of UPF-PSO-SVR in 5# was 0.0011, which was the smallest value in the comparison results. The MSE value in 6# was 0.0007. The RMSE value in battery 7# was 0.022. The results show that the UPF-PSO-SVR model has higher accuracy in capturing real changes in battery capacity degeneration. In contrast, the traditional regression model and the neural network model have higher prediction error and MSE value under the same conditions. Moreover, the prediction error distribution of UPF-PSO-SVR model is more concentrated. Most of the error values are close to

Table 1 Initial settings of model parameters

No	B0005	B0006	B0007	B0018
a	1.98	1.57	1.96	1.86
b	−0.002719	−0.005576	−0.002098	−0.002917
c	−0.1697	0.489	−0.0971	0.0002
d	−0.0694	0.0009	−0.0971	0.0002
T/Cycle	60	60	60	40
C	79.58	33.48	35.26	97.16
K	RBF			
γ	0.04287	0.06483	0.05891	0.01819

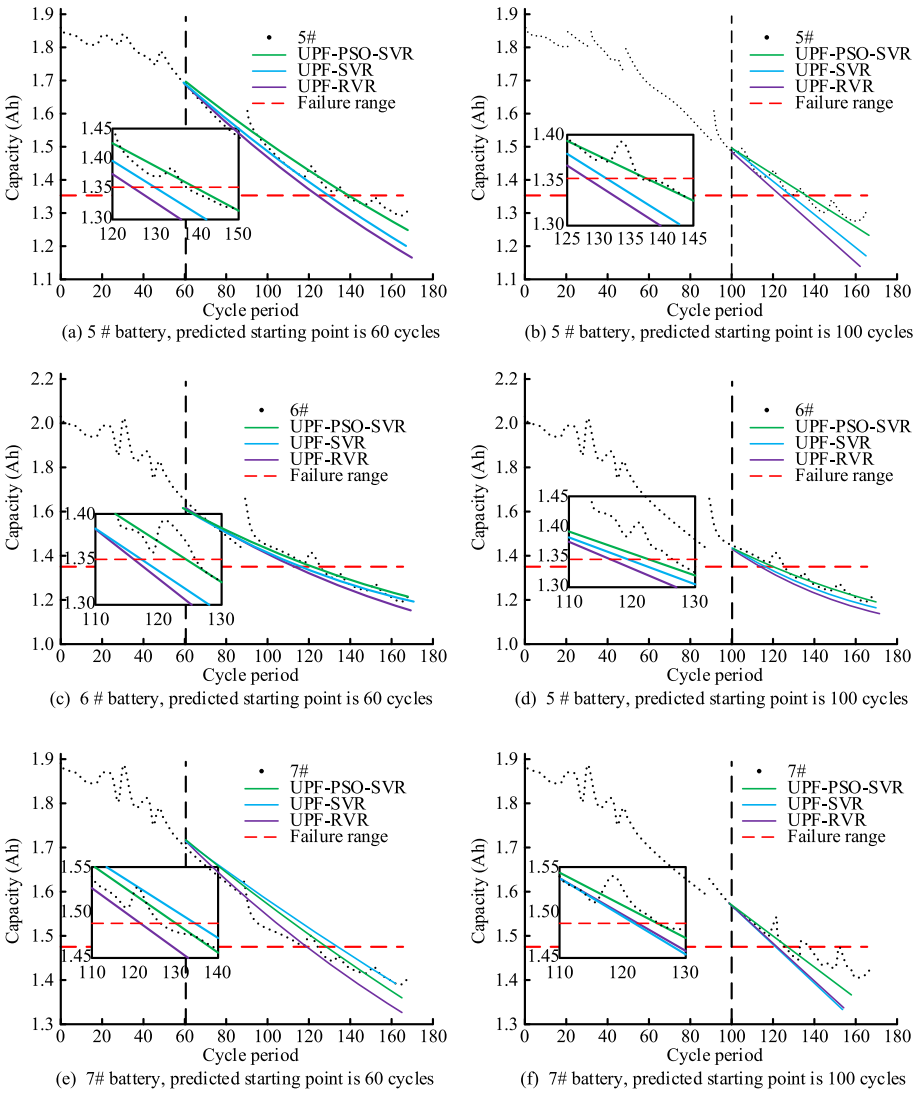

(a) 5 # battery, predicted starting point is 60 cycles
(b) 5 # battery, predicted starting point is 100 cycles
(c) 6 # battery, predicted starting point is 60 cycles
(d) 5 # battery, predicted starting point is 100 cycles
(e) 7# battery, predicted starting point is 60 cycles
(f) 7# battery, predicted starting point is 100 cycles

Fig. 5 Comparison of the prediction effects of each model on batteries

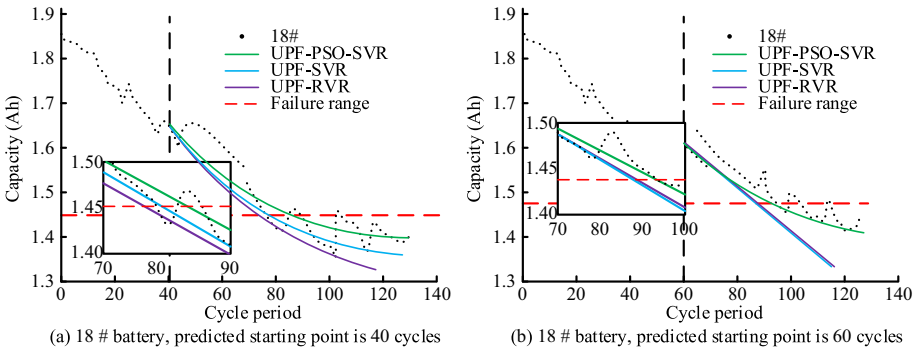

(a) 18 # battery, predicted starting point is 40 cycles
(b) 18 # battery, predicted starting point is 60 cycles

Fig. 6 Prediction effect of each model on 18# battery

zero, while the error distribution of other models is more scattered, and there are more extreme error values. This further proves the superiority of UPF-PSO-SVR model in dealing with complex datasets and non-linear relationships. The prediction performance of battery 18# is shown in Fig. 6.

In Fig. 6, UPF-PSO-SVR had the smallest RMSE among all models, with a value of 0.0013. The prediction curve of UPF-PSO-SVR model still followed the actual capacity decline curve. The prediction results show that UPF-PSO-SVR model can maintain consistent prediction accuracy and stability under different test conditions. This further demonstrates the advantages of the UPF-PSO-SVR in predicting battery capacity degradation, verifying the robustness and wide adaptability of the UPF-PSO-SVR model.

Uncertainty and error analysis of prediction results

To discuss the uncertainty and error, the study selects the B0005 battery from the NASA dataset for uncertainty analysis. The study evaluates the prediction performance by predicting the PH and the convergence index of the algorithm. The life prediction results and PH performance results of different prediction algorithms for different prediction beginning points are shown in Fig. 7.

In Fig. 7, the lifetime prediction and PH prediction using the UPF-PSO-SVR algorithm were superior to the UPF-RVR and UPF-SVR algorithms. For the PH results, the error of UPF-PSO-SVR model reached the allowable range when the battery charge and discharge cycle was 50cycle. The prediction error of UPF-RVR model reached the allowable range at 80cycle. The prediction error of UPF-SVR model reached the allowable range at 70cycle. The results show that the UPF-PSO-SVR model has excellent performance in predicting real battery data, both short-term and long-term prediction. The convergence index of the model is shown in Fig. 8.

In Fig. 8, the convergence of the UPF-PSO-SVR was better than that of UPF-RVR and UPF-SVR. From the convergence results, the UPF-PSO-SVR had lower convergence at earlier prediction cycles. In later prediction, the convergence speed of the UPF-PSO-SVR was faster and more stable. The fast convergence shows that the model can

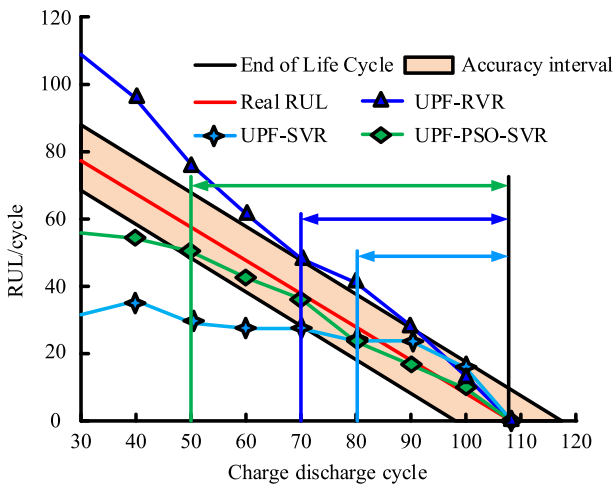

Fig. 7 Life prediction and PH of various algorithms at various prediction beginning points

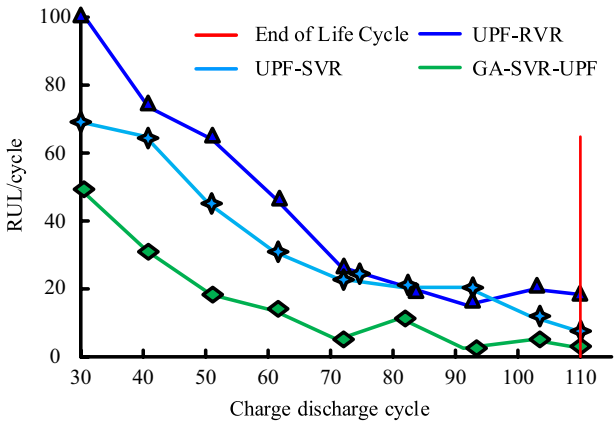

Fig. 8 Convergence indicators of different prediction methods

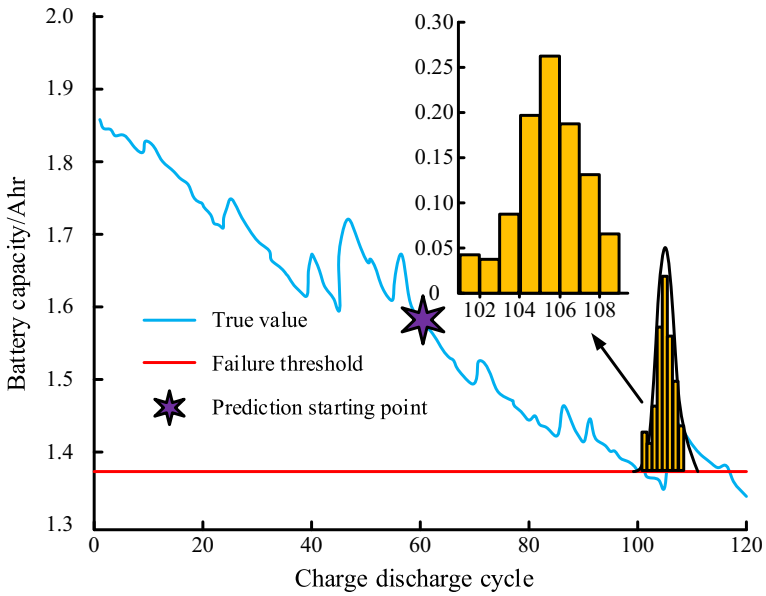

Fig. 9 Histogram of probability distribution of prediction results

achieve high prediction accuracy in a short time, saving training time and computing resources. The stable convergence ensures that the model can achieve consistent performance under different operating environments and conditions, avoiding fluctuation and instability in the training process. As for the uncertainty of the model prediction results, in the study, a histogram is used to represent the probability distribution of measurement results. It clearly displays the probability density distribution of type prediction errors. By observing the probability distribution of prediction errors, the performance of the UPF-PSO-SVR model in different prediction error ranges is more obvious. The high density region indicates that the model appears more frequently in this error range, reflecting the centrality and reliability of the model prediction. The result of the probability distribution histogram is shown in Fig. 9.

Table 2 Comparison results of calculation efficiency of the model

Evaluation index	Running time (s)	Memory usage (MB)	Processor utilization (%)
UPF-SVR	182.4	153.2	80
UPF-RVR	203.3	164.7	85
UPF-PSO-SVR	217.6	181.4	90

Table 3 Prediction errors of the model for different types of batteries

Battery type	Evaluation index	UPF-PSO-SVR	PSO-SVR	UPF-SVR
Nickel metal hydride battery	MSE	0.0015	0.0023	0.002
	MAE	0.0048	0.0071	0.0065
Lithium iron phosphate battery	MSE	0.0013	0.0021	0.0017
	MAE	0.0045	0.0067	0.0058
Lithium titanate battery	MSE	0.0011	0.0018	0.0014
	MAE	0.004	0.0059	0.0052

Figure 9 shows the probability distribution of the end of battery life cycle. The true battery capacity degradation was around 105 cycles, and the prediction starting point was 60 cycles. In the histogram of the prediction results, the highest probability of predicting the end of life cycle was 105 cycles, with a probability value of 28.18%. In order to weigh the calculation effect of the model, the running time, memory usage and processor utilization of the model are analyzed through comparative experiments. The results were shown in Table 2.

In Table 2, for the UPF-SVR model, the running time, memory usage, and processor utilization were 182.4s, 153.2 MB, and 80%, respectively. For the UPF-RVR model, the running time, memory usage, and processor utilization were 203.3 s, 164.7 MB and 85%, respectively. UPF-PSO-SVR model was 217.6s, 181.4 MB, and 90%, respectively. The results show that the proposed UPF-PSO-SVR model has higher computational resource requirements and running time in terms of computational efficiency, which is due to the complex computational process combining PSO optimization and UPF filtering. However, despite the high computing resource requirements, the UPF-PSO-SVR model shows significant advantages in prediction accuracy and stability. It provides more accurate and reliable technical support for capacity decline management and health assessment of lithium-ion batteries. In order to test the performance of UPF-PSO-SVR model on different types of batteries, the study selects three different types of batteries to carry out capacity decline prediction experiments, including nickel metal hydride batteries, lithium iron phosphate batteries and lithium titanate batteries. Carried out capacity decline prediction experiments. The results are shown in Table 3.

In Table 3, the UPF-PSO-SVR model haf better prediction performance than the PSO-SVR and UPF-SVR models on different battery types. It demonstrates that the designed method has strong adaptability on different battery types. UPF-PSO-SVR model can be easily expanded and adjusted due to its modular structure. For different types

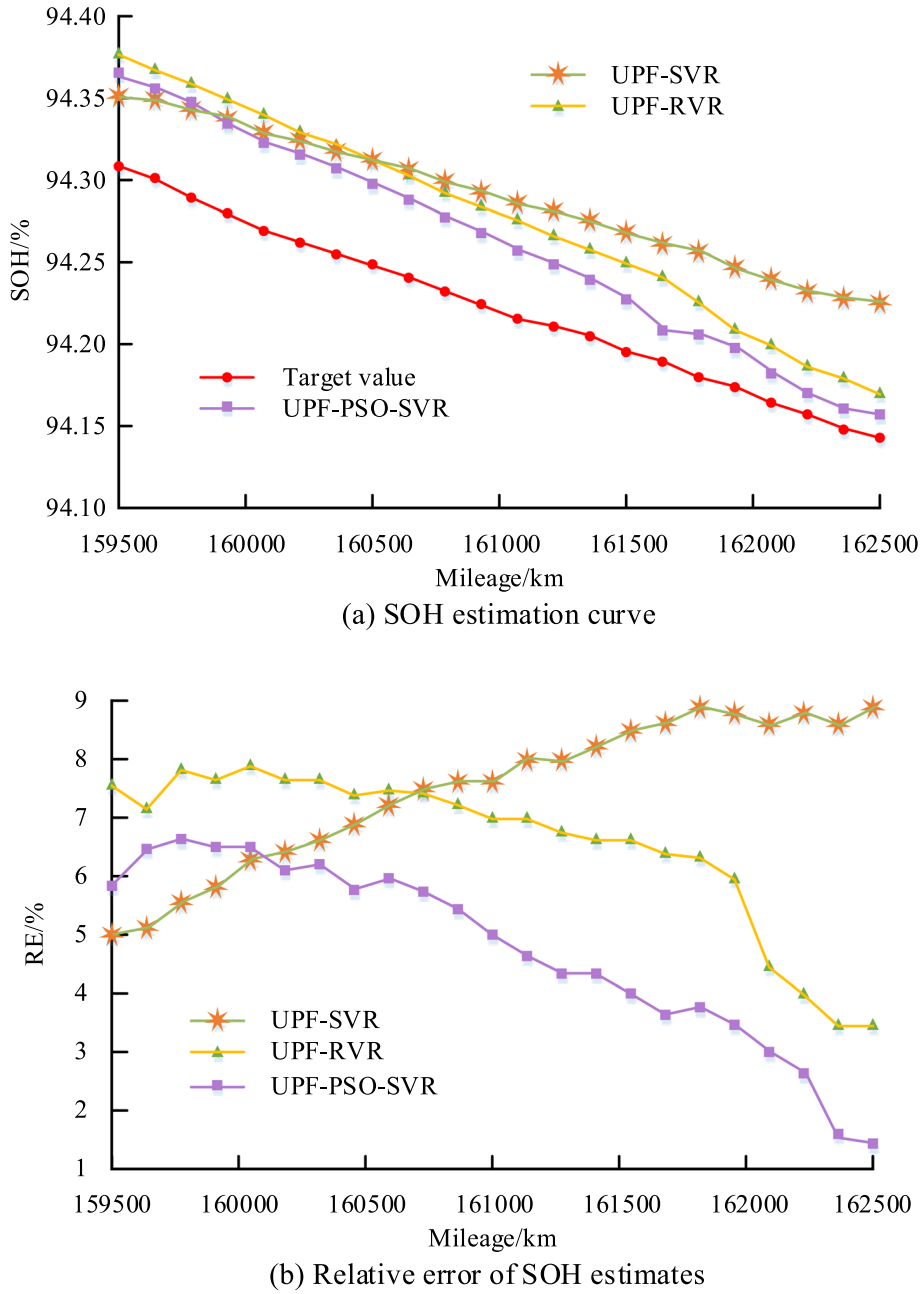

Fig. 10 Actual test results of different models

of batteries, the model parameters and data preprocessing methods only need to be adjusted according to the characteristics of the specific battery. The research continues to verify the prediction accuracy and reliability of the proposed model through practical tests. In this study, the new energy vehicle data collected by BMS is used as experimental data. The electric vehicle in the data is lithium iron phosphate, and the collection frequency is 20s/ times. The data includes total vehicle mileage, vehicle status information, as well as total battery voltage, total current, maximum temperature, minimum

temperature, and SOC. The model is tested using this data and evaluated by battery State of Health (SOH) and Relative Error (RE). The results are shown in Fig. 10.

In Fig. 10a, the SOH estimation curves of UPF-SVR model and UPF-RVR model had roughly the same variation trend. The SOH estimation results continued to approximate the true value with the advance of time series. The prediction results of UPF-PSO-SVR model were closer to the target value. The results verify the validity of UPF-PSO-SVR model for SOH estimation. From Fig. 10b, the RE of the three models in the early stage of SOH estimation was approximately the same, among which UPF-SVR model was the lowest. As the battery is used, the RE of SOH estimation was gradually reduced. Finally, the RE value was only 1%.

Among the above results, the proposed model achieves low SOH error. At present, the existing errors are mainly systematic errors. Specifically, improper model parameter settings prevent the model from fully learning the nonlinear characteristics of battery performance changes. Because the battery performance has very complex changes, the model can not fully learn the law of battery degeneration, which leads to certain systematic errors. It is not susceptible to systematic error in short-term prediction, but has a certain impact on long-term prediction. However, under sufficient data conditions, the model can still control the prediction error within a reasonable range.

Health testing of LB

To prove the effects of health characteristics on the SOH evaluation results, Shapley values of various features are obtained. The absolute Shapley values of all feature points within the class are taken. Then the average Shapley values of various health features are obtained to characterize the influence of health features on SOH evaluation results. The test results are shown in Fig. 11.

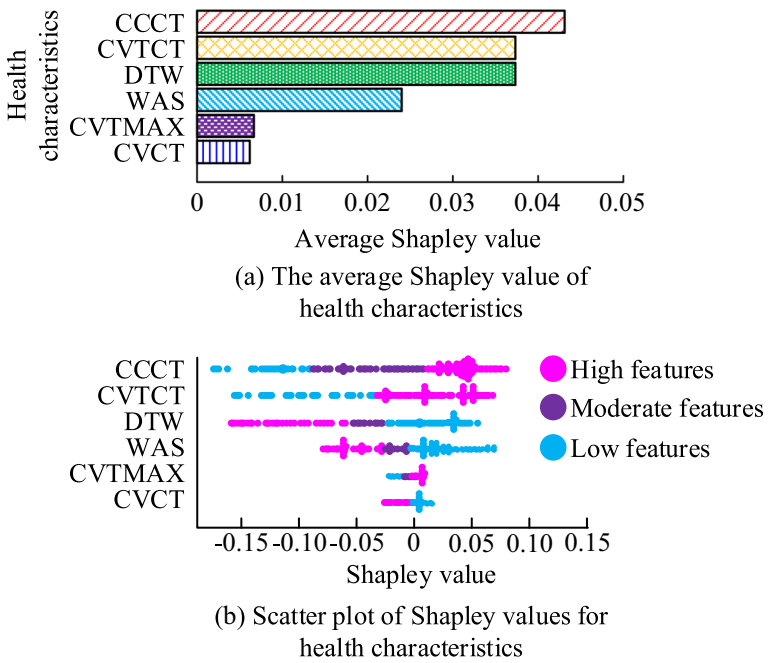

Fig. 11 Summary of shapley values for health characteristics

Figure 11a shows the average Shapley values of battery health characteristics. The results showed that the average Shapley values of Constant Current Charge Time (CCCT), Constant Voltage Transition Charge Time (CVTCT), Discharge Time Window (DTW), and Weighted Average State (WAS) were higher. Therefore, these four types of features were considered as key health characteristics of batteries. Figure 11b shows the battery health characteristics. The highest Shapley of CCCT was around 0.08, while the lowest Shapley value of DTW was −0.16. CCCT and CVTCT have a positive impact on battery SOH. With the increase of characteristic values, the Shapley value increases, corresponding to a higher battery SOH. Battery SOH was negatively affected by DTW and WAS. As the characteristic values increase, the Shapley value gradually decreases, corresponding to a lower battery SOH. However, other health characteristics have a relatively small impact on battery SOH. By averaging the Shapley value, the study was able to quantify the influence of each feature on the model prediction results. A higher Shapley value indicates that the feature contributes more to the model prediction. A lower Shapley value indicates that the feature contributes less. More in-depth data mining and processing can be carried out for features with greater contribution. For features with low contribution, the dimensionality can be reduced or the data quality can be optimized

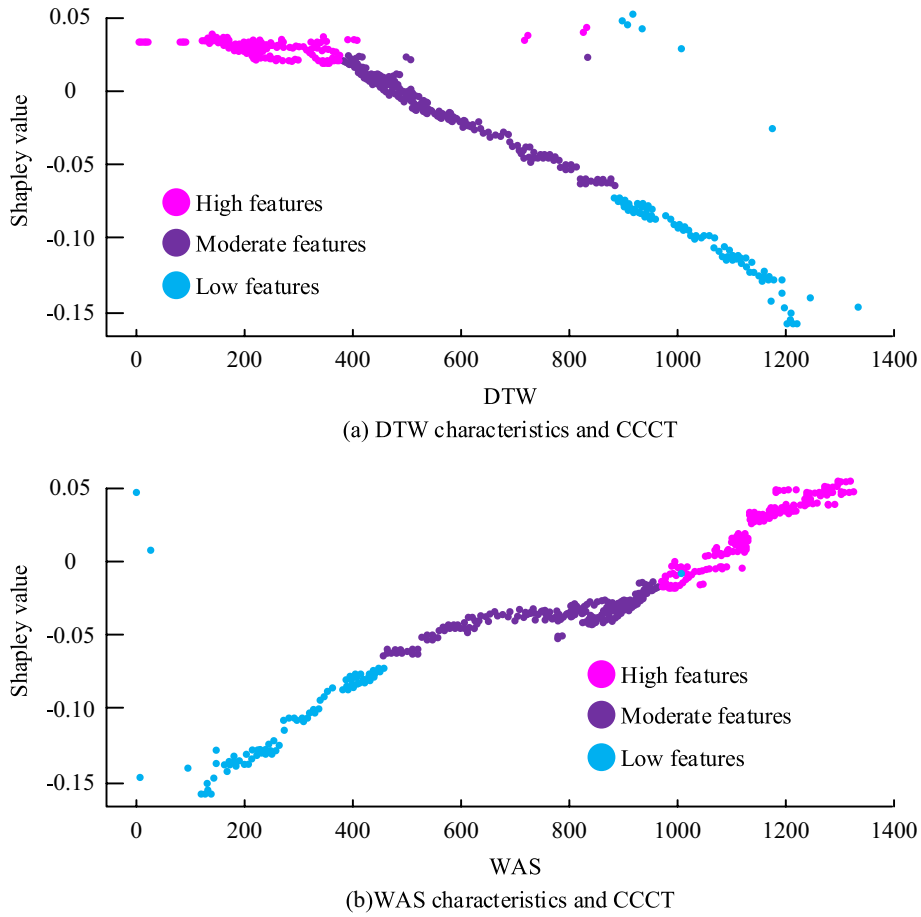

Fig. 12 Dependencies for key health characteristics

to improve the overall performance of the model. The study analyzes the evaluation between health characteristics and battery SOH. Figure 12 presents the results.

Figure 12a shows the Shapley value variation of DTW and its relationship with CCCT features. When the DTW eigenvalue was less than 400, the Shapley value was positive, which had a positive impact on the SOH evaluation results. With the increase of DTW eigenvalues and the decrease of CCCT eigenvalues, there was a significant negative correlation between them. Figure 12b shows the Shapley value variation of CVTCT and its relationship with CCT features. When the change of constant voltage charging voltage remained stable for more than 5000 s, the Shapley value turned positive. It had a positive impact on the SOH evaluation results. With the increase of stable duration, the duration of constant voltage charging increased synchronously, showing a positive correlation between them. Key health features reveal the importance and impact of features on battery health prediction through the interaction and correlation between features. Some characteristics may have a greater impact on predicted outcomes under certain conditions and less impact under others. The interaction between dependency and key health features helps to understand the complex contribution of features to prediction results. In summary, it can accurately predict the remaining life of batteries. It can provide comprehensive feature analysis and performance testing for battery health. The experimental results show that the non-linear and non-Gaussian noise problems of the system are dealt with by UPF. The reliability of the data and the robustness of the model are significantly improved. Compared with traditional filtering algorithms, UPF can more accurately capture the noise characteristics of battery capacity changes, thus reducing prediction errors. SVR uses kernel function technique to deal with complex non-linear relationship, which can better reflect the real change of battery capacity decline. PSO algorithm optimizes the parameter combination of SVR through global search. Therefore, SVR can find the optimal kernel function parameter and regularization parameter in the high-dimensional parameter space. This optimization process improves the prediction accuracy of the model.

Through the above comparative analysis, the UPF-PSO-SVR model shows significant advantages in predicting the capacity decline of lithium-ion batteries. The model is significantly better than the centralized comparison model in the performance indicators such as MSE and MAE, showing a high prediction accuracy. However, higher computing resource requirements, including longer running time and higher memory and processor usage, reflect the complexity of the model. In terms of implementation difficulty, the UPF-PSO SVR model is more complex, but its adaptability is strong. It can effectively deal with complex non-linear relations and data noise, which is suitable for a variety of different battery types and scenarios. Therefore, the UPF-PSO-SVR model shows important practical value in applications requiring high prediction precision.

Conclusion

In vehicles powered by new energies, the stability and safety of battery performance are one of the most critical technical challenges. Especially, the battery capacity degradation has a direct impact on the service life of batteries and the performance of the entire vehicle. The LB detection model based on UPF-PSO-SVR was built for testing LB. This model combined the particle filtering and PSO technology. Then the remaining life and

the health characteristics of batteries were analyzed through SVR. Experiments were carried out on 5#, 6#, 7#, and 18#. In the 5# battery test, the UPF-PSO-SVR model was able to reduce RMSE to 0.0011. In predicting 18# battery, the RMSE was reduced to 0.0013. From the analysis of model uncertainty and error, the model had good stability and accuracy. In the analysis of health characteristics, the results showed that CCCT and CVTCT positively affected battery SOH, while Battery SOH negatively affected by DTW and WAS. The UPF-PSO-SVR was effective and accurate in predicting battery capacity degradation, providing an effective technical means for capacity degradation management and health assessment. The main contribution of the research is to improve the reliability of the data and the robustness of the model. Therefore, the model can show higher stability and consistency when processing the actual battery data. The prediction accuracy of the model is improved, so that it can maintain high precision prediction under different battery types and usage conditions. The prediction performance of SVR is significantly improved, especially in the high-dimensional parameter space, which ensures the superior performance of the model under various complex conditions. Through the innovative combination of UPF, PSO and SVR, the ability to process noisy data, capture nonlinear relationships, and optimize parameter settings is enhanced. Although it has achieved certain results, there are still some limitations. For example, in order to reduce the influence of external factors on the experimental results, the research tries to maintain the consistency of the experimental environment as much as possible, thus lacking discussion and analysis of the external environment. In future research, a detailed analysis of the impact of external factors on battery performance will be conducted. At the same time, the model structure is further simplified to improve algorithm efficiency and explore parameter adjustment strategies applicable to a wider range of battery types.

Author contributions
Hongxing Liu wrote the main manuscript text and Yi Liang revised the manuscript critically. Both authors reviewed this manuscript.

Funding
The research is supported by 2023 Guangxi Zhuang Autonomous Region Young and Middle Aged Teachers Basic Ability Enhancement Project-Design and Research of a Power Battery Active Passive Hybrid Balance System Based on Microcontrollers, Project Number: 2023KY0817.

Availability of data and materials
All data generated or analyzed during this study are included in this article.

Declarations

Ethics approval and consent to participate
Not applicable.

Consent for publication
Not applicable.

Competing interests
There's no competing interests.

Received: 1 April 2024 Accepted: 19 June 2024
Published online: 26 June 2024

References

Cao H, Wu Y, Bao Y, Feng X, Wan S, Qian C (2023) UTrans-net: a model for short-term precipitation prediction. Artif Intell App 1(2):106–113

Che Y, Hu X, Lin X, Guo J, Teodorescu R (2023) Health prognostics for lithium-ion batteries: mechanisms, methods, and prospects. Energy Environ Sci 16(2):338–371

Du K, Liu M, Zhou J, Khandelwal M (2022) Investigating the slurry fluidity and strength characteristics of cemented backfill and strength prediction models by developing hybrid GA-SVR and PSO-SVR. Min Metal Explor 39(2):433–452

Guo X, Wang K, Yao S, Fu G, Ning Y (2023) RUL prediction of lithium ion battery based on CEEMDAN-CNN BiLSTM model. Energy Rep 9(1):1299–1306

Hu T, Ma H, Liu K, Sun H (2022) Lithium-ion battery calendar health prognostics based on knowledge-data-driven attention. IEEE Trans Industr Electron 70(1):407–417

Kong D, Wang S, Ping P (2022) State-of-health estimation and remaining useful life for lithium-ion battery based on deep learning with Bayesian hyperparameter optimization. Int J Energy Res 46(5):6081–6098

Liu K, Peng Q, Sun H, Fei M, Ma H, Hu T (2022) A transferred recurrent neural network for battery calendar health prognostics of energy-transportation systems. IEEE Trans Industr Inf 18(11):8172–8181

Ma G, Xu S, Jiang B, Cheng C, Yang X, Shen Y, Yang T, Huang Y, Ding H, Yuan Y (2022) Real-time personalized health status prediction of lithium-ion batteries using deep transfer learning. Energy Environ Sci 15(10):4083–4094

Mao L, Zhao J, Zhu Y, Chen J (2022) A noise-immune model identification method for lithium-ion battery using two-swarm cooperative particle swarm optimization algorithm based on adaptive dynamic sliding window. Int J Energy Res 46(3):3512–3528

Meng J, Azib T, Yue M (2023) Early-Stage end-of-Life prediction of lithium-Ion battery using empirical mode decomposition and particle filter. Proc Inst Mech Eng Part A J Power Energy 237(5):1090–1099

Nsugbe E (2023) Toward a self-supervised architecture for semen quality prediction using environmental and lifestyle factors. Artif Intell App 1(1):35–42

Pervaiz S, Bangyal WH, Ashraf A, Kashif N, Muhammad RH, Chowdhry BS et al (2022) Comparative research directions of population initialization techniques using PSO algorithm. Intell Autom Soft Comput 32(3):1427–1444

Ra N, Dutta A, Bhattacharjee A (2022) Optimizing vanadium redox flow battery system power loss using particle swarm optimization technique under different operating conditions. Int J Energy Res 46(12):17346–17361

Sevilgen G, Bulut E, Albak ES et al (2022) Prediction and optimization of the design decisions of liquid cooling systems of battery modules using artificial neural networks. Int J Energy Res 46(6):7293–7308

Sun H, Yang D, Du J, Li P, Wang K (2022) Prediction of Li-ion battery state of health based on data-driven algorithm. Energy Rep 8(1):442–449

Xiong R, Sun Y, Wang C, Tian J, Chen X, Li H, Zhang Q (2023) A data-driven method for extracting aging features to accurately predict the battery health. Energy Storage Mater 57(2):460–470

You H, Zhu J, Wang X, Jiang B, Sun H, Liu X et al (2022) Nonlinear health evaluation for lithium-ion battery within full-lifespan. J Energy Chem 72(5):333–341

Zhang Y, Zhao M (2023) Cloud-based in-situ battery life prediction and classification using machine learning. Energy Storage Mater 57(2):346–359

Zhang C, Wang S, Yu C (2022) Novel improved particle swarm optimization-extreme learning machine algorithm for state of charge estimation of lithium-ion batteries. Ind Eng Chem Res 61(46):17209–17217

Zhi Y, Wang H, Wang L (2022) A state of health estimation method for electric vehicle Li-ion batteries using GA-PSO-SVR. Complex Intell Syst 8(3):2167–2182

Publisher's Note